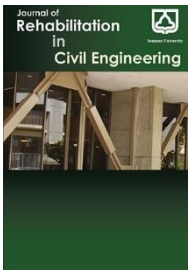

journal homepage: http://civiljournal.semnan.ac.ir/

Study on Linear and Nonlinear Dynamically P-Delta Effects on Frame Structures under Earthquake Spectra, Harmonic and Stochastic Excitations

Dana Afshar[1] , Majid Amin Afshar[2]

1. PhD Candidate, Department of Technology and Engineering, Imam Khomeini International University, P.O. Box 34149-16818, Qazvin, Iran
2. Assistant Professor, Department of Technology and Engineering, Imam Khomeini International University, P.O. Box 34149-16818, Qazvin, Iran
Corresponding author: mafshar@eng.ikiu.ac.ir

ARTICLE INFO

Article history:
Received: 06 May 2020
Revised: 19 September 2020
Accepted: 20 January 2021

Keywords:
Dynamic analysis;
P-delta effects;
multiple scales method;
Stochastic excitation;
Earthquake Spectrum.

ABSTRACT

In this research the effect of axial load on dynamic behavior of a simple frame, subjected to harmonic, seismic and earthquake excitation has been studied. The differential equations of motion have been considered for two types of small and large deformations. The method of multiple scales has been applied to solve the differential equations of motion with harmonic loading and for small and large deformations. Then, the steady state response near one-to-one resonance condition has been studied and the effect of axial force in resonance and non-resonance conditions has been investigated, which has not been considered before. It is clear from the results that the dynamic behavior of the frame under axial load is completely different in resonance and non-resonance cases and the axial load has respectively descending and ascending effects on the responses in resonance and non-resonance conditions. The equations of motion under earthquake loading are also considered and the time history and the response spectrum of the model show that the axial load has increased the responses under earthquake excitation. Although white noise as a stochastic loading is applied to the model and, the results are approximated using the method of stochastic differential equations so, the mean value and covariance are calculated and the effect of axial force on them is investigated.

1. Introduction

The study of axial load effect on the response of the structures and investigating the stability of the systems is one of the most important subjects in structural engineering. Considering axial load effect in dynamic behavior of the structures leads to

How to cite this article:
Afshar, D., Amin Afshar, M. (2021). Study on Linear and Nonlinear Dynamically P-delta Effects on Frame Structures under earthquake spectra, harmonic and stochastic excitations. Journal of Rehabilitation in Civil Engineering, 9(3), 75-88.
https://doi.org/10.22075/jrce.2021.19323.1365

appear the nonlinearity in the differential equations of motion. In order to study these nonlinear differential equations the perturbation method has been used in this study. Most of the researchers study the effect of axial load and p-delta effects statically. Bagci [1] has presented the elastic stability analysis and buckling loads of beams, shafts and frames on elastic foundations. Moreover, Melaibari et al. [2] have studied Static stability of higher order functionally graded beams under variable axial load. Frame structural systems that include column and beam elements, are known as the most common structures in civil engineering. Lee et al. [3] have investigated large deflections of rectilinear frames under arbitrary discrete loads. Various studies have considered P-delta effects by modifying the stiffness matrix. Rutenberg [4] has evaluated the effect of p-delta on plane frame structures with negative stiffness using nonlinear computer program. Moreover, Wilson and Habibullah [5] have represented an algorithm to incorporate the p-delta effects in the structural stiffness matrix for static and dynamic analysis. Also, some researchers interested in dynamic stability, and studied the behavior of the systems subjected to harmonic and seismic loading. According to Bolotin's definition, the mechanical systems exhibit a specific dynamic stability of motion [6]. Instability effects of vertical motion of foundation on the 2D elastic frames have been studied by Zingone and Muscolino [7]. Dynamic stability of a rotating sandwich beam with magnetorheological elastomer core has been studied by Nayak et al. [8]. Sakar et al. [9] searched stability of frames with several spans under periodic forces. Aydınoğlu and Fahjan [10] have surveyed the p-delta effect on inelastic behavior of SDOF systems under seismic excitation. Lopez et al. [11] have represented a new seismic design method considering p-delta effects for framed structures under seismic excitation. Also the effect of axial force in dynamic analysis of structures is appeared in stiffness matrix, which has been attained by Chen [12] for a flexible beam with axial force. It is important to note that considering axial load by assuming large deflections for simple shear frames under harmonic excitation, results in nonlinear differential equations. So the method of multiple scales is applied to derive the response of the differential equations. Studying nonlinear differential equations by perturbation method and finding resonance conditions is an important section of this paper. Nayfeh and Balachandran [13] discussed on nonlinear modal interactions of harmonically excited structures among theoretical and experimental research. Afaneh and Ibrahim [14] have evaluated the nonlinear response of an initially buckled beam under harmonic excitation using multiple scales method. Also, the dynamically P-delta effects under earthquake and stochastic loading have been investigated in this paper. Moreover it is necessary to study structures under stochastic loading which leads to the stochastic differential equations because of the stochastic nature of the earthquake. These differential equations have been solved using the method represented by Sarkka and Solin [15]. An overwhelming works have devoted to the response of the mechanical systems to stochastic and random Excitation [16-24]. We should note that none of the works have been mentioned above investigated the p-delta effect under internal and external resonances and there are no searches about the behavior of the

systems under stochastic excitation considering axial forces. In this paper the behavior of a simple shear frame under harmonic excitation while p-delta effects have been considered, has been evaluated in resonance and non-resonance cases in section 3. Also, the response of the frame under stochastic excitation has been investigated in section 4. In section 5 the dynamic effects of axial load under earthquake excitation is studied and the numerical examples have been presented in section 6 and the results have been compared with those acquired using multiple scales method.

2. General equations of motion

Consider a frame structural system with single floor and single span, as shown in the Fig. (1), excited by a harmonic or earthquake lateral force and axial forces acting on the columns. The mass of the system is intensive on the nodes as shown in figure. The equations of motion of the system in x and y directions considering axial force according to Chen [12] are as bellow

$$m_x\ddot{x} + c_x\dot{x} + k_x\phi_1 x = F \tag{1}$$

$$m_y\ddot{y} + c_y\dot{y} + k_y y = 0 \tag{2}$$

where m is the mass of the system, k_x and k_y are stiffnesses in x and y directions, c is the damping coefficient, F is the lateral force and ϕ_1 is a coefficient for considering the effect of axial force and is defined as follows

$$\phi_1 = \frac{(k_x L)^3 \sin(k_x L)}{12(2 - 2\cos(k_x L) - kL\sin(k_x L))} \tag{3}$$

k_x and k_y are defined as follows

$$k_x = \frac{12EI}{L_0^3} \tag{4}$$

$$k_y = \frac{AE}{L_0} \tag{5}$$

and the frequencies in x and y directions are

$$\omega_x = \sqrt{\frac{k_x}{m_x}}, \omega_y = \sqrt{\frac{k_y}{m_y}} \tag{6}$$

By assuming m= m_x and m_y and substituting Eqs. (4)-(6) into Eqs. (1) and (2) and subsequently dividing by m, the following simpler equations are obtained as follow

$$\ddot{x} + 2\xi_x\omega_x\dot{x} + \phi_1\omega_x^2 x = \frac{F}{m} \tag{7}$$

$$\ddot{y} + 2\xi_y\omega_y\dot{y} + \omega_y^2 y = 0 \tag{8}$$

3. Harmonic excitation

In this part, a uniformly valid solution of Eqs. (7) and (8) has been obtained using multiple scales method. Here we consider three types of analysis, small axial force and small deformation, small axial force and large deformation, and large axial force. First, we study the model with small axial force and small deformation. It is assumed that the lateral force is harmonic force, *i.e.* $F=A.sin(\omega t)$, where ω and A are excitation frequency and amplitude. The following non-dimensional variables are defined as

$$\Omega = \frac{\omega}{\omega_x}, \Omega_y = \frac{\omega_y}{\omega_x}, \tau = \omega_x t$$

$$X = \frac{x}{L_0}, Y = \frac{y}{L_0} \tag{9}$$

which L_0 is the length of the column before deformation and because of considering small deformation in this section, the length of the column after deformation is assumed

to be equal to the length of the column before deformation.

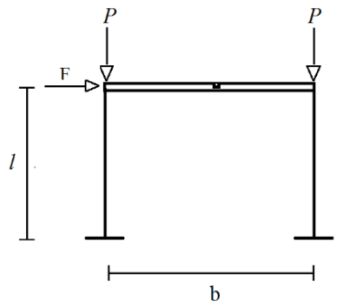

Fig. 1. Simple frame with rigid beam.

Substituting the above terms into Eqs. (7) and (8) the non-dimensional differential equations are as bellow

$$\ddot{X} + 2\xi_x \dot{X} + \phi_1 X = \frac{A}{mL_0\omega_x^2}\sin(\Omega\tau) \tag{10}$$

$$\ddot{Y} + 2\xi_y \dot{Y} + \Omega_y^2 Y = 0 \tag{11}$$

The Taylor series of ϕ_1 is

$$\phi_1 \approx 1 - \frac{(kL)^2}{10} - \frac{(kL)^4}{8400} \tag{12}$$

which k is defined as

$$k = \sqrt{\frac{P}{EI}} \tag{13}$$

P is the axial force and $P_e = \frac{\pi^2 EI}{L_0^2}$is the Euler critical axial load. Substituting Eq. (13) into Eq. (12) results in

$$k^2 \times \frac{\pi^2}{\pi^2} \times \frac{L_0^2}{L_0^2} = \frac{P}{P_e} \times \frac{\pi^2}{L_0^2} \rightarrow k^2 L_0^2 = \pi^2 \frac{P}{P_e} \tag{14}$$

$$\phi_1 \approx 1 - \frac{\pi^2}{10}\frac{P}{P_e} - \frac{\pi^2}{8400}(\frac{P}{P_e})^2 \tag{15}$$

The fraction P/P_e is a dimensionless quantity, hereinafter referred to as the axial load ratio.

Now two time variables T_0 and T_1 are introduced as$T_0 = \varepsilon^0\tau$ and $T_1 = \varepsilon^1\tau$. They scale real time τ to fast and slow independent times, respectively and ε is a dimensionless parameter. Then, according to Nayfeh [25] and by using chain rule, the derivatives with respect to τ are transformed to the new variables as follow

$$\frac{d}{d\tau} = D_0 + \varepsilon D_1 + \varepsilon^2 D_2 \tag{16}$$

$$\frac{d^2}{d\tau^2} = (D_0 + \varepsilon D_1 + \varepsilon^2 D_2)(D_0 + \varepsilon D_1 + \varepsilon^2 D_2) = D_0^2 + 2\varepsilon D_0 D_1 + \ldots \tag{17}$$

where $D_k = \partial/\partial T_k$. Then, the approximations of the small parameters X and Y have been assumed as bellow

$$X = X_0 + \varepsilon X_1 + \varepsilon^2 X_2 + \ldots \qquad Y = Y_0 + \varepsilon Y_1 + \varepsilon^2 Y_2 + \ldots \tag{18}$$

Since the motions in vicinity of the static position are assumed small and conventional structural systems experience little damping, it makes sense that the damping ratio and also the amplitude of the harmonic force and the axial load ratio can be ordered as

$$\xi_x = \varepsilon\xi_x, A = \varepsilon D, \frac{P}{P_e} = \varepsilon P \tag{19}$$

Substituting Eqs. (15) - (19) into Eqs. (10) and (11) and then gathering and leveling out terms with like powers of ε, the following equations are obtained:

$$o(\varepsilon^0): D_0^2 X_0 + X_0 = 0 \tag{20}$$

$$o(\varepsilon^1): D_0^2 X_1 + X_1 = D\sin(\Omega\tau) + \frac{1}{10}P\pi^2 X_0 - 2D_0 D_1 X_0 - 2\xi_x D_0 X_0 \tag{21}$$

The general solution of Eq. (20) is as follows

$$X_0 = A_x(T_1)\exp(iT_0) + cc \tag{22}$$

where cc is the complex conjugate of the previous term. Substituting Eq. (22) into Eq. (20) gives

$$D_0^2 X_1 + X_1 = -2iA_x' \exp(iT_0) + \frac{\pi^2}{10} PA_x exp(iT_0) + Dsin(\Omega\tau)$$
$$= -2iA' exp(iT_0) + \frac{\pi^2}{10} PA_x exp(iT_0) + \frac{iD}{2}(exp(-i\Omega T_0) - exp(i\Omega T_0)) - 2i\xi_x A_x exp(iT_0) \quad (23)$$

which $'$ shows the differentiation with respect to T_0. Evaluating the second-order approximate solutions has shown that an external resonance can occur. The resonance conditions are complied with ratios, $\Omega \approx 1$, leads to the second-order approximate solution containing secular terms. By approaching the external excitation frequency, ω to ω_x, external resonance condition will be provided. To describe the proximity of the excitation frequency to the external resonance conditions, the following detuning parameter, σ, are defined

$$\Omega = 1 + \varepsilon\sigma \quad (24)$$

Eliminating secular terms results in

$$-2iA_x' + \frac{\pi^2}{10} PA_x - \frac{iD}{2} exp(i\sigma T_1) - 2i\xi_x A_x = 0 \quad (25)$$

The solution of Eq. (25) is as follow

$$A_x = \frac{1}{2} a_x exp(i\beta_x) \quad (26)$$

where a_x is a complex constant. Substituting Eq. (26) into Eq. (25) and separating the real and imaginary parts we obtain

$$(\frac{\pi^2}{20} P + \sigma) a_x + \frac{D}{2} sin(\lambda) = 0$$
$$a_x' + a_x \xi_x + \frac{D}{2} cos(\lambda) = 0 \quad (27)$$

which λ is defined as $\lambda = \sigma T_1 - \beta_x$. The steady state solution of the above equations is obtained by setting $a_x' = \lambda' = 0$.

$$a_x = \frac{(D/2)}{\sqrt{\xi_x^2 + (\frac{\pi^2}{20} P + \sigma)^2}} \quad (28)$$

$$x = \frac{DL}{2\sqrt{\xi_x^2 + (\frac{\pi^2}{20} P + \sigma)^2}} cos(\omega t + arctg(\frac{\frac{\pi^2}{20} P + \sigma}{\xi_x})) \quad (29)$$

Eq. (29) shows that the effect of axial load on the lateral deformation in the external resonance case is similar to the effect of damping and helps to reduce the deformation.

3.1. Small axial force and large deformations

In this section the deformation of the system is assumed to be large, so as it can be seen from Fig. (2) that the length of the columns changed after deformation and it can be calculated by considering lateral and axial deformation of the column. By using the perturbation method the nonlinear differential equations considering large deformations have been solved. The length of the column after deformation is as follows

$$L^2 = (L_0 + y)^2 + x^2$$
$$L = L_0 \sqrt{(1 + (\frac{y}{L_0}))^2 + (\frac{x}{L_0})^2} \quad (30)$$

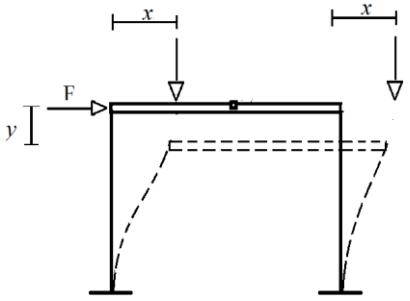

Fig. 2. Deformation of the frame with rigid beam.

which *l* is defined as

$$l=\sqrt{(1+(\frac{y}{L_0}))^2+(\frac{x}{L_0})^2} \tag{31}$$

The differential equation in the x direction is

$$\ddot{x}+2\xi_x\omega_x\dot{x}+\phi_1\frac{12EI}{mL_0^3}\times\frac{1}{l^3}x=\frac{A}{m}\sin(\omega t) \tag{32}$$

The ϕ_1 coefficient depends on the length of the column, so it must be modified considering the deformation and changing the length of the column.

$$\begin{aligned}\phi_1&=1-\frac{(kL)^2}{10}\times\frac{L_0^2}{L_0^2}-\frac{(kL)^4}{8400}\times\frac{L_0^4}{L_0^4}\\&=1-\frac{(kL_0)^2}{10}l^2-\frac{(kL_0)^4}{8400}l^4\end{aligned} \tag{33}$$

$$\phi_1=1-\frac{\pi^2}{10}\frac{P}{P_e}l^2-\frac{\pi^2}{8400}(\frac{P}{P_e})^2l^4 \tag{34}$$

The differential equation in the x direction after substituting Eq. (34) and subdividing the equation by l is

$$\begin{aligned}&\ddot{X}+2\xi_x\dot{X}+(\frac{1}{l^3}-\frac{\pi^2}{10}\frac{P}{P_e}\frac{1}{l}-\frac{\pi^2}{8400}(\frac{P}{P_e})^2l)X\\&=\frac{A}{mL_0\omega_x^2}\sin(\Omega\tau)\end{aligned} \tag{35}$$

The stiffness in the y direction is also modified as follow

$$k_y=\frac{AE}{L}\frac{L_0}{L_0}=\frac{AE}{L_0}\frac{1}{l} \tag{36}$$

The differential equation in the y direction after substituting Eq. (36) and subdividing the equation by l is

$$\ddot{Y}+2\xi_y\dot{Y}+\frac{\Omega_y^2}{l}y=0 \tag{37}$$

The parameters l^{-1}, l^{-3} and l are estimated by their Tailor series as bellow

$$\begin{aligned}l^{-1}&=1-\frac{1}{2}\varepsilon(X^2+2Y+Y^2)\\l^{-3}&=1-\frac{3}{2}\varepsilon(X^2+2Y+Y^2)\\l&=1+\frac{1}{2}\varepsilon(X^2+2Y+Y^2)\end{aligned} \tag{38}$$

After substituting Eqs. (38) into Eqs. (32) and (37) and using multiple scales method to solve the equations in x and y directions and, then leveling out terms with like powers of ε, the following differential equations are acquired as

$$\begin{aligned}&o(\varepsilon^0):D_0^2X_0+X_0=0\\&o(\varepsilon^0):D_0^2Y_0+\Omega_y^2Y_0=0\end{aligned} \tag{39}$$

$$\begin{aligned}&o(\varepsilon^1):D_0^2X_1+X_1=D\sin(\Omega\tau)+\frac{1}{10}P\pi^2X_0\\&-2D_0D_1X_0-2\xi_xD_0X_0+\frac{3X_0^3}{2}+3X_0Y_0+\frac{3}{2}X_0Y_0^2\\&o(\varepsilon^1):D_0^2Y_1+\Omega_y^2Y_1=-2D_0D_1Y_0-2\xi_yD_0Y_0\\&+\frac{1}{2}\Omega_y^2X_0^2Y_0+\Omega_y^2Y_0^2+\frac{1}{2}\Omega_y^2Y_0^3\end{aligned} \tag{40}$$

The solutions of Eqs. (39) are as follows

$$\begin{aligned}X_0&=A_x(T_1)\exp(iT_0)+cc\\Y_0&=A_y(T_1)\exp(i\Omega_yT_0)+cc\end{aligned} \tag{41}$$

Substituting Eqs. (41) into Eqs. (40) gives

$$\begin{aligned}&D_0^2X_1+X_1=Dsin(\Omega\tau)+1/10p\pi^2(A_xexp(iT_0)+\bar{A}_xexp(-iT_0))\\&-2i\xi_xA_xexp(iT_0)+2i\xi_x\bar{A}_xexp(-iT_0)-2i\frac{dA_x}{dT_1}exp(iT_0)\\&+2i\frac{d\bar{A}_x}{dT_1}exp(-iT_0)+\frac{3}{2}(3A_x^2\bar{A}_xexp(iT_0)+3A_x\bar{A}_x^2exp(-iT_0))\\&+\frac{3}{2}(A_xA_y^2exp(iT_0(1+2\Omega_y)+A_x\bar{A}_y^2exp(iT_0(1-2\Omega_y))\\&+2A_xA_y\bar{A}_yexp(iT_0)+\bar{A}_xA_y^2exp(-iT_0(1-2\Omega_y))\\&+2\bar{A}_xA_y\bar{A}_yexp(-iT_0)))+NST\end{aligned} \tag{42}$$

$$\begin{aligned}&D_0^2Y_1+\Omega_y^2Y_1=-2i\Omega_y\frac{dA_y}{dT_1}exp(i\Omega_yT_0)+2i\Omega_y\frac{d\bar{A}_y}{dT_1}exp(-i\Omega_yT_0)\\&-2i\Omega_y\xi_yA_yexp(i\Omega_yT_0)+2i\Omega_y\xi_y\bar{A}_yexp(-i\Omega_yT_0)\\&+\frac{1}{2}\Omega_y^2(A_y\bar{A}_x^2exp(iT_0(\Omega_y-2))+2A_yA_x\bar{A}_xexp(i\Omega_yT_0)\\&+\bar{A}_yA_x^2exp(-iT_0(\Omega_y-2))+2A_x\bar{A}_yexp(-i\Omega_yT_0))\\&+\frac{1}{2}\Omega_y^2(3A_y^2\bar{A}_y\bar{A}_xexp(i\Omega_yT_0)+3A_y\bar{A}_y^2exp(-i\Omega_yT_0))+NST\end{aligned} \tag{43}$$

which NST are non-secular terms. The second-order approximate solutions show that both internal and external resonances can occur simultaneously. The resonance conditions are complied with ratios, $\Omega_y = \Omega = 1$, result in the reduced second-order approximate solution containing secular terms. The internal resonance condition is provided by approaching the natural frequency in the horizontal direction, i.e. ω_x, to the natural frequency in vertical direction, ω_y. Also in the external resonance situation, the excitation frequency, ω, is close to ω_x. To explain how the frequencies are close to the resonance condition, detuning parameters are defined as follow

$$\begin{aligned} &1-2\Omega_y = -1 \rightarrow \Omega_y = 1+\varepsilon\sigma_1 \\ &\Omega = 1+\varepsilon\sigma_2 \end{aligned} \tag{44}$$

where σ_1 and σ_2 are the detuning parameters for internal and external resonances, respectively. The solution of Eqs. (42) and (43) leads to the following equations

$$\begin{aligned} &A_x = \frac{1}{2} a_x exp(i\beta_x) \\ &A_y = \frac{1}{2} a_y exp(i\beta_y) \end{aligned} \tag{45}$$

Substituting Eq. (45) into Eqs. (42) and (43) and separating the real and imaginary parts leads to a system of autonomous ordinary differential equations in polar form

$$\begin{aligned} &-\frac{da_x}{dT_1} - \frac{D}{2}cos(\lambda_2) - \xi_x a_x + \frac{3}{16} a_x a_y^2 sin(\lambda_1) = 0 \\ &\frac{d\beta_x}{dT_1} a_x + \frac{D}{2} sin(\lambda_2) + \frac{1}{20} p\pi^2 a_x + \frac{9}{16} a_x^3 + \frac{3}{8} a_x a_y^2 + \frac{3}{16} a_x a_y^2 cos(\lambda_1) = 0 \\ &-\Omega_y \frac{da_y}{dT_1} - \Omega_y \xi_y a_y - \frac{1}{16} \Omega_y^2 a_y a_x^2 sin(\lambda_1) = 0 \\ &\Omega_y \frac{d\beta_y}{dT_1} a_y + \frac{1}{8} \Omega_y^2 a_y a_x^2 + \frac{1}{16} \Omega_y^2 a_y a_x^2 cos(\lambda_1) + \frac{3}{16} \Omega_y^2 a_y^3 = 0 \end{aligned} \tag{46}$$

which λ_1 and λ_2 are defined as follow

$$\begin{aligned} &2\sigma_1 T_1 + 2\beta_y - 2\beta_x = \lambda_1 \\ &\sigma_2 T_1 - \beta_x = \lambda_2 \end{aligned} \tag{47}$$

Steady state solution of Eqs. (46), by setting $\frac{da_x}{dT_1} = 0, \frac{da_y}{dT_1} = 0, \frac{d\lambda_1}{dT_1} = 0$ and $d\lambda_2/dT_1 = 0$ leads to the following equation

$$\begin{aligned} &a_y = 0 \rightarrow \frac{D^2}{4} - \frac{81a_x^6}{256} + a_x^4\left(-\frac{9p\pi^2}{160} - \frac{9\sigma_2}{8}\right) \\ &+a_x^2\left(-\frac{1}{400} p^2\pi^4 - \xi_x^2 - \frac{1}{10} p\pi^2\sigma_2 - \sigma_2^2\right) = 0 \end{aligned} \tag{48}$$

By solving Eq. (48) in section 4 and comparing the results with exact solution of equations of motion, the accuracy of the perturbed solution is investigated.

3.2. Large axial force

In this part, the effect of large axial load ratio, disregarding whether the deformations are big or small, is investigated and it is assumed that P/P_e is closely near 1, so after substituting this relation into Eq. (10) and using multiple scales method to solve the resulted differential equation and then leveling out terms with like powers of ε, the differential equations are acquired as follow

$$\begin{aligned} &o(\varepsilon^0): D_0^2 X_0 + X_0\left(1 - \frac{\pi^2}{10} - \frac{\pi^4}{8400}\right) = 0 \\ &o(\varepsilon^1): D_0^2 X_0 + X_1\left(1 - \frac{\pi^2}{10} - \frac{\pi^4}{8400}\right) = \\ &Dsin(\Omega\tau) - 2D_0 D_1 X_0 - \frac{1}{10}\pi^2 X_0 p' - \frac{\pi^4 X_0 p'}{4200} \end{aligned} \tag{49}$$

Because of the small quantity of $(1 - \pi^2/10 - \pi^4/8400)$ it can be equal to ε

$$1 - \frac{\pi^2}{10} - \frac{\pi^4}{8400} = \varepsilon \tag{50}$$

Substituting Eq. (50) into Eq. (49), the result of solving the first order equation is as follow

$$X_0 = AT_0 + B \tag{51}$$

Substituting Eq. (51) into Eq. (49) results in

$$D_0^2 X_1 = -(AT_0 + B) + D\sin(\Omega\tau) - \frac{1}{20}\pi^2 (AT_0 + B)^3 + \frac{\pi^4 (AT_0 + B)^3}{16800} - 2D_0 D_1 (AT_0 + B) + \frac{3}{2}(AT_0 + B)^3 - \frac{1}{10}\pi^2 (AT_0 + B)p' - \frac{\pi^4}{4200}(AT_0 + B)p' \quad (52)$$

Solving Eq. (52) is possible by using the bellow initial condition

$$X(0) = 0, X'(0) = 0 \quad (53)$$

The lateral deformation of the system is then, acquired as bellow

$$X = \frac{A}{mL_0\Omega\omega_x} t - \frac{A}{mL_0\Omega^2\omega_x} \sin(\Omega t) \quad (54)$$

4. Stochastic excitation

Since the earthquake can be accounted as stochastic loading, by the method of stochastic differential equation we can achieve an approximate solution of the differential equation of motion of the frame. The equation of motion of the frame under stochastic loading is as follows

$$\ddot{x} + 2\xi_x \dot{x} + (1 - \frac{\pi^2}{10}\frac{P}{P_e})x = w(t) \quad (55)$$

which $w(t)$ is a Gaussian white noise. Gaussian white noise is a weakly stationary process that is delta-correlated and zero mean. The above differential equation is written in state-space model as bellow

$$\begin{bmatrix} \dot{x}_1 \\ \dot{x}_2 \end{bmatrix} = \begin{bmatrix} 0 & 1 \\ -(1 - \frac{\pi^2}{10}\frac{P}{P_e}) & -2\xi_x \end{bmatrix} \begin{bmatrix} x_1 \\ x_2 \end{bmatrix} + w(t) \begin{bmatrix} 0 \\ 1 \end{bmatrix} \quad (56)$$

$$\frac{dx}{dt} = Fx + Lw(t) \quad (57)$$

The steady state solution of the above SDE is

$$\frac{dm(t)}{dt} = Fm(t) = 0 \quad (58)$$

$$\frac{dR}{dt} = FR(t) + R(t)F^T + LQL^T = 0 \quad (59)$$

which m is the mean value vector, R is the covariance matrix and Q is the spectral density of $w(t)$. By solving the above matrix equations

$$m = \begin{bmatrix} 0 \\ 0 \end{bmatrix} \quad (60)$$

$$R = \begin{bmatrix} \frac{q}{4\xi(1 - \frac{\pi^2}{10}\frac{P}{P_e})} & 0 \\ 0 & \frac{q}{4\xi} \end{bmatrix} \quad (61)$$

The general solution of the above equation is as bellow

$$R(t) = \begin{bmatrix} R_{11}(t) & R_{12}(t) \\ R_{21}(t) & R_{22}(t) \end{bmatrix} \quad (62)$$

$$\frac{dR}{dt} = FR(t) + R(t)F^T + LQL^T \quad (63)$$

$$\frac{d}{dt}\begin{bmatrix} R_{11}(t) & R_{12}(t) \\ R_{21}(t) & R_{22}(t) \end{bmatrix} = \begin{bmatrix} a & b \\ c & d \end{bmatrix} \quad (64)$$

which *a, b, c* and *d* are defined as bellow

$$\begin{aligned} a &= R_{12} + R_{21} \\ b &= R_{22} - (1 - \frac{\pi^2}{10}\frac{P}{P_e})R_{11} - 2\xi_x R_{12} \\ c &= -(1 - \frac{\pi^2}{10}\frac{P}{P_e}) \\ d &= q - (1 - \frac{\pi^2}{10}\frac{P}{P_e})R_{12} - 4\xi_x R_{22} - (1 - \frac{\pi^2}{10}\frac{P}{P_e})R_{21} \end{aligned} \quad (65)$$

By solving the differential Eqs. (64) the equations of R_{11}, R_{12}, R_{22} and R_{21} which are the covariance matrix elements are obtained.

Table 1. Characteristics of the models

Model	h(cm)	m(kg)	A(cm^2)	E(kg/cm^2)	I(cm^4)	ξ_x	P
1	400	200	400	2×10^6	1.333×10^4	0.05	0.02
2	400	2500	50	2×10^6	6.65×10^5	0.05	0.02

Table 2. Characteristics of the earthquakes

Field	Earthquake Name	Magnitude	Station Name	Year	Ys30	PGA	Rup(km)	RSN
Far	BAM	6.6	Abaragh	2003	412.23	0.77g	47.18	4037
	KOBE	6.9	Chihaya	1995	609	0.52g	49.91	1102
	MANJIL	7.37	Qazvin	1990	302.64	0.89g	49.97	1636
	NORTHWEST	5.9	Xiker	1997	341.56	0.2g	52.36	1749
	SOUTHERN CALIFORNIA	6	San Luis Obispo	1952	493.5	0.22g	73.41	17
	TABAS	7.35	Ferdows	1978	302.64	0.41g	91.14	140
	TOTTORI	6.61	HRS003	2000	335.55	0.55g	65.81	3872
Near	BAM	6.6	Bam	2003	487.4	3.74g	1.7	4040
	KOBE	6.9	KJMA	1995	312	3.42g	0.96	1106
	MANJIL	7.37	Abbar	1990	723.95	2.51g	12.55	1633
	NORTHWEST	6.1	Jiashi	1997	240.09	1.19g	17.73	1752
	SANFERNADO	6.61	Pacoima Dam	1971	2016.13	3.8g	1.81	77
	TABAS	7.35	Tabas	1978	766.77	4.85g	2.05	143
	TOTTORI	6.61	SMN015	2000	616.55	1.02g	9.12	3943

5. Earthquake excitation

To evaluate the dynamic effect of axial force on a frame structure under earthquake excitation, a real earthquake record, Kobe 1995, is applied to the structure and the time history response is assessed for different values of the axial force for the proposed model.

Fig. (3) shows the time history of Kobe's earthquake, and Fig. (4) shows the time history of the model. We can see that as the value of axial force is increased the response of the system becomes bigger.

5.1. Response spectra of the frame v.s axial load

This section is devoted to find the response spectra of the model 1 under 7 far and 7 near earthquakes which for the far and near earthquakes respectively the distance from the fault is assumed to be more and smaller than 20 km . Then the effect of axial force on the response spectrum is surveyed. Table. 2 shows the characteristics of the earthquakes. In this table Ys30 is the velocity of shear wave in the depth of 30 meters, PGA is the maximum acceleration of the earth, and Rup is the distance from the fault. Figs. (5) and (7) shows the response spectra of the frame with axial load ratios smaller than 0.1 for far and near-fault earthquakes respectively. Figs. (6) and (8) shows the response spectra for axial load ratios bigger than 0.1. It can be seen from the figures that the axial load causes increasing the response of the frame in almost whole range of periods of the model. It is also concluded from the figures that for

axial load ratio smaller than 0.1 its effect on the responses is negligible however it is clear from the figures that the effect of the axial load ratios bigger than 0.1 is noticeable and can't be neglected, especially for structural periods smaller than 0.6 sec.

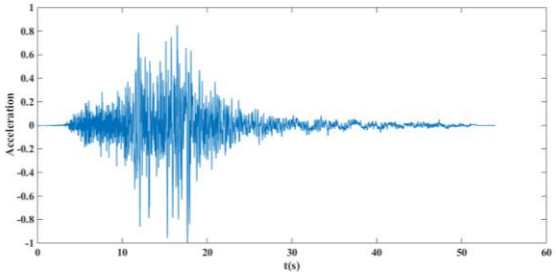

Fig. 3. Kobe earthquake time history.

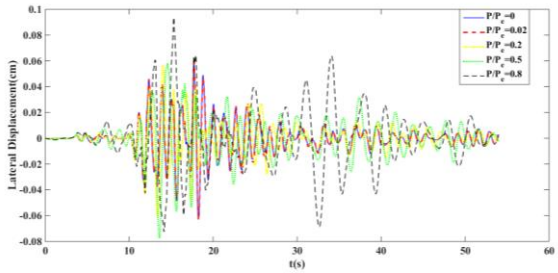

Fig. 4. Time history of the frame for various axial load ratios.

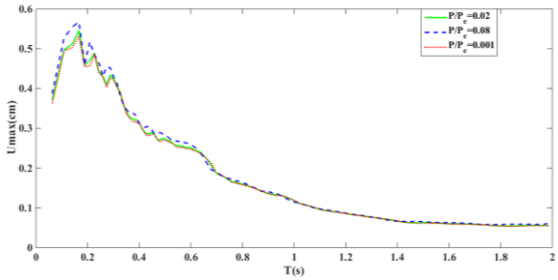

Fig. 5. Response spectra of the frame for axial load ratios smaller than 0.1 for far earthquakes.

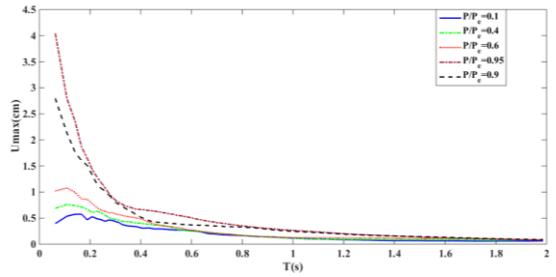

Fig. 6. Response spectra of the frame for axial load ratios bigger than 0.1 for far earthquakes.

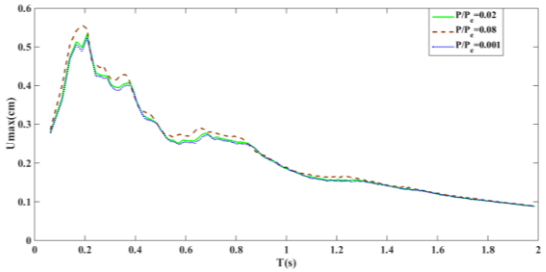

Fig. 7. Response spectra of the frame for axial load ratio smaller than 0.1 for near earthquakes.

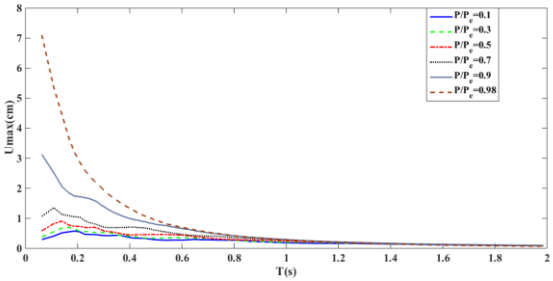

Fig. 8. Response spectra of the frame for axial load ratio bigger than 0.1 for near earthquakes.

6. Numerical results

In this part, we first study the responses of the proposed model to harmonic forces and earthquake excitations when the frame imposed to small or large values of axial forces and deformations. A time history analysis under Kobe 1995 earthquake has been done. The maximum acceleration is scaled up to 1.0g. several amplitudes are selected for the harmonic excitations and the frequency is tuned to the first lateral natural frequency of the structure.

The time histories are attained based on solving Eqs. (10) and, (11), numerically, by means of ODE45 solver in the MATLAB 2014. To gain the numerical solutions of the perturbation analysis, the software package MATHEMATICA 10.0 has been used.

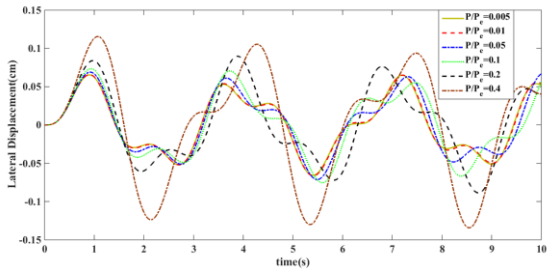

Fig. 9. Axial load effect on the lateral displacement under non-resonance condition.

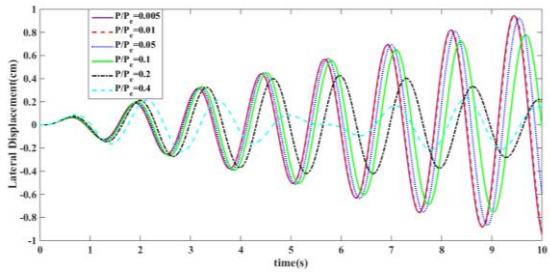

Fig. 10. Axial load effect on the lateral displacement under resonance condition.

6.1. Harmonic excitation

The external harmonic excitation frequency, and the natural frequency in x direction are away from each other in the non-resonance case. Fig. (9) represents the lateral displacement of the frame with respect to time for the linear model (1) for different values of axial forces and constant damping ratio, $\xi_x = 0.05$ in non-resonance condition. In this case, by increasing the axial force, lateral displacements increase and so the axial load has an opposite behavior as damping, so growing axial force increases the probability of structural instability. Furthermore, it can be seen from the Fig. (9) that because of the difference between the natural frequency and the excitation frequency, more than one peak exist in the amplitude of motion with respect to time.

The next case complies with the ratios $\omega_x \approx \omega \approx 1$, which is the resonance case. Fig. (10) shows the lateral displacement with respect to time for different values of axial load ratios under resonance condition. It has been shown that the effect of axial load is like the effect of damping and causes decreasing the lateral displacement. Fig. (11) shows a comparison between approximated solution of Eq. (29), and the numerical exact solution of Eq. (10) and as it can be seen from the figure, an acceptable conformity exists particularly for $P/P_e < 0.8$. Beyond $P/P_e = 0.1$, a fast drop in lateral deformation is seen by increasing the value of axial force and whatever the value of axial load ratio becomes bigger than 0.1, the severity of decreasing the response is reduced and almost for $0.2 < P/P_e < 0.9$ the response dependence to axial force is disappeared. For $P/P_e > 0.9$, the structural function is close to the unstable situation and a fast jump is seen in the graph.

For large deformations Eq. (48) is solved by MATHEMATICA and the lateral motion amplitude has been acquired and the results compared with exact results in Fig. (12). Also the numerical solution of equation of motion, ignoring large deformations has been done. A good coincidence between the perturbed solution and the exact solution can be seen from the figure and it is clear from the figure that the results of Eq. (48) is closed to the numerical results which has been obtained considering large deformations.

To study the effect of big axial force ($P/P_e > 0.9$), numerical solution of Eq. (10) has been done and the result is compared with Eq. (54) which, is acquired from perturbation solution. The results have been shown in Fig. (13) and it can be deduced from the figure that, when the axial force is near the critical buckling load, the stability of the system is influenced, the system becomes unstable and the response increases dramatically.

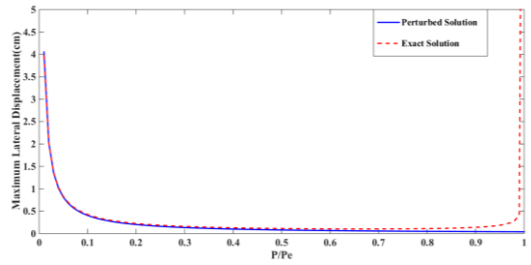

Fig. 11. The effect of axial force on the lateral displacement under lateral harmonic excitation and resonance condition.

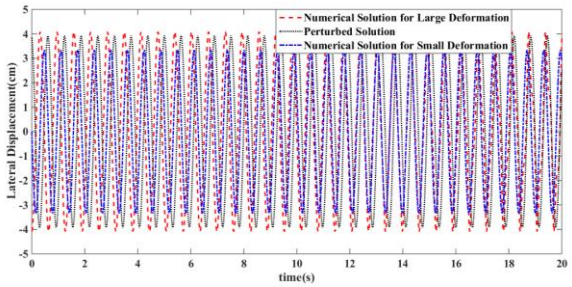

Fig. 12. Axial load effect on the lateral displacement under resonance condition in the case of large deformations.

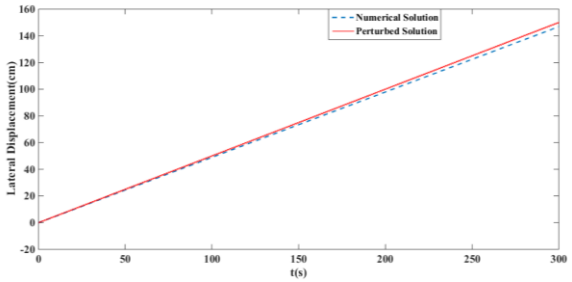

Fig. 13. Effect of big axial load on the lateral displacement of the frame.

6.2. Stochastic loading

The system of differential equations acquired by SDE method as [62] is numerically solved for model (1) by MATLAB, and the results are shown as the figures bellow. Figs. (14), (16) and (18) respectively, shows the effect of axial load on R_{11}, R_{12} and R_{22}. From Figs. (14) and (16) one can conclude that, as the value of axial force increased the quantity of R_{11} and R_{12} increased too and the peaks of the curvatures shifted to right side of the diagram by the time. It is obvious that these increase and shift of the peaks are evident specially for the axial load ratios bigger than 0.1. The effect of axial force on R_{22} just shift the phase of the curvatures and doesn't affect the values of R_{22} by the time. Figs. (15), (17) and (19) respectively, shows the effect of damping on R_{11}, R_{12} and R_{22}. It is obvious from the figures that the axial load has an converse effect with damping and causes increasing the response of the frame.

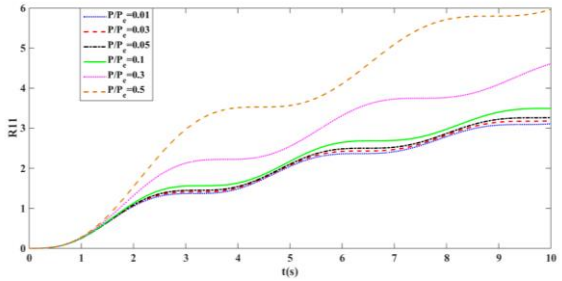

Fig. 14. Axial load effect on R_{11}

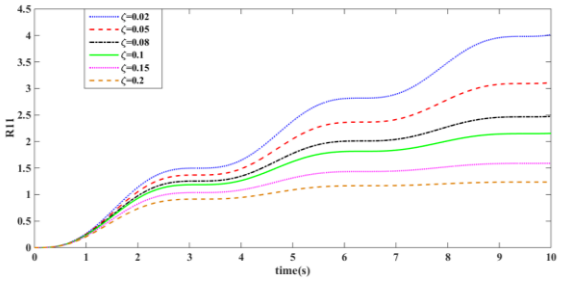

Fig. 15. Damping effect on R_{11}

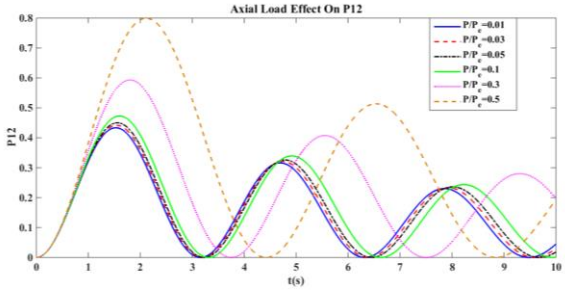

Fig. 16 Axial load effect on R_{12}

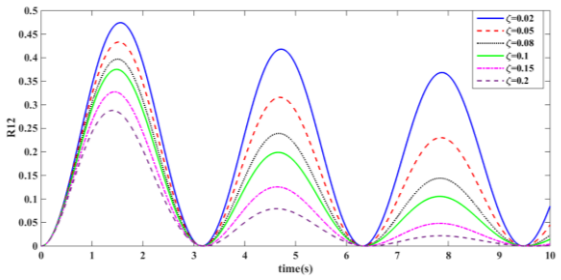

Fig. 17. Damping effect on R_{12}

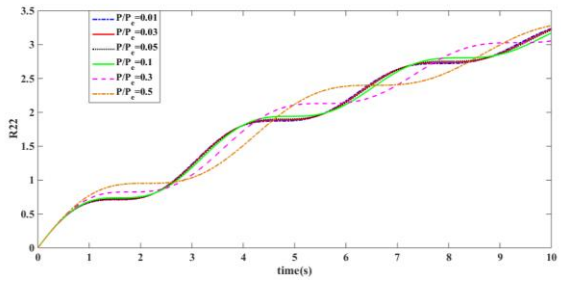

Fig. 18. Axial load effect on R_{22}

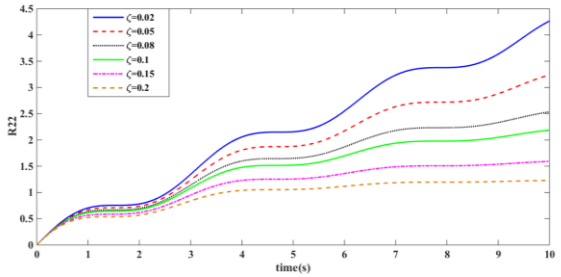

Fig. 19. Damping effect on R_{22}

7. Conclusions

In this paper a simple frame is modeled and the P-delta effect on the dynamic analysis of the frame under harmonic, seismic and stochastic load is investigated. The governing differential equations of motion are formulated. The outcome of the results of dynamic analysis of the frame is as follows:

From perturbation analysis based on the multiple scales method, it was obtained that for small amounts of axial load and deformation, the axial load has the same descending performance as damping to the structural response under external resonance condition. In the non-resonance condition, the axial load behaves inversely and increasing it increases the structural responses.

Under large axial force the system becomes unstable and the response of the system dramatically increased by the time.

Under stochastic loading, the effect of damping and axial load on the elements of the covariance matrix is investigated. It is concluded that the effect of damping are the same on all of the elements of the covariance matrix and as the amount of damping increases, the amount of covariance matrix elements decreases. The effect of axial force on the matrix elements is a little different. It has an ascending effect on R_{11} and R_{12} but its effect is neutral on the R_{22} and just causes shifting in phase.

Under earthquake excitation the effect of axial force is as it is expected and increases the response of the system.

References

[1] Bagci, C. (1980). Elastic stability and buckling loads of multi-span nonuniform beams, shafts and frames on rigid or elastic supports by finite element method using planar uniform line elements. Computers & Structures, 12(2), 233-243.

[2] Melaibari, A., Abo-bakr, R. M., Mohamed, S. A., & Eltaher, M. A. (2020). Static stability of higher order functionally graded beam under variable axial load. Alexandria Engineering Journal, 59(3), 1661-1675.

[3] Lee, S. L., Manuel, F. S., & Rossow, E. C. (1968). Large deflections and stability of elastic frame. Journal of the Engineering Mechanics Division, 94(2), 521-548.

[4] Rutenberg, A. (1981). A direct P-delta analysis using standard plane frame computer programs. Computers & Structures, 14(1-2), 97-102.

[5] Wilson, E. L., & Habibullah, A. (1987). Static and dynamic analysis of multi-story

buildings, including P-delta effects. Earthquake spectra, 3(2), 289-298.

[6] Bolotin, V. V. (1962). THE DYNAMIC STABILITY OF ELASTIC SYSTEMS. VOLUME 2. AEROSPACE CORP EL SEGUNDO CA.

[7] Zingone, G., & Muscolino, G. (1982). Dynamic stability of plane elastic frames. Journal of Sound and Vibration, 85(3), 397-406.

[8] Nayak, B., Dwivedy, S. K., & Murthy, K. S. R. K. (2014). Dynamic stability of a rotating sandwich beam with magnetorheological elastomer core. European Journal of Mechanics-A/Solids, 47, 143-155.

[9] Şakar, G., Öztürk, H., & Sabuncu, M. (2012). Dynamic stability of multi-span frames subjected to periodic loading. Journal of Constructional Steel Research, 70, 65-70.

[10] Aydınoğlu, M. N., & Fahjan, Y. M. (2003). A unified formulation of the piecewise exact method for inelastic seismic demand analysis including the P-delta effect. Earthquake engineering & structural dynamics, 32(6), 871-890.

[11] López, S. E., Ayala, A. G., & Adam, C. (2015). A novel displacement-based seismic design method for framed structures considering P-Delta induced dynamic instability. Bulletin of Earthquake Engineering, 13(4), 1227-1247.

[12] Chen, W. K. (2018). Stability design of steel frames. CRC press.

[13] Nayfeh, A. H., & Balachandran, B. (1989). Modal interactions in dynamical and structural systems.

[14] Afaneh, A. A., & Ibrahim, R. A. (1993). Nonlinear response of an initially buckled beam with 1: 1 internal resonance to sinusoidal excitation. Nonlinear Dynamics, 4(6), 547-571.

[15] Särkkä, S., & Solin, A. (2019). Applied stochastic differential equations (Vol. 10). Cambridge University Press.

[16] Solomos, G. P., & Spanos, P. D. (1984). Oscillator response to nonstationary excitation.

[17] Kiureghian, A. D. (1981). A response spectrum method for random vibration analysis of MDF systems. Earthquake Engineering & Structural Dynamics, 9(5), 419-435.

[18] Heredia-Zavoni, E., & Vanmarcke, E. H. (1994). Seismic random-vibration analysis of multisupport-structural systems. Journal of Engineering Mechanics, 120(5), 1107-1128.

[19] Patil, A. E., & Bhanuse, M. M. (2020). Seismic Analysis of Eccentric Steel Structure on a Shaking Table. Computational Engineering and Physical Modeling, 3(2), 1-11. https://doi.org/10.22115/cepm.2020.223528.1093

[20] Bakhshi, H., Khosravi, H., & Ghoddusi, M. (2019). Evaluation of seismic behavior of steel shear wall by time history analysis. Computational Engineering and Physical Modeling, 2(1), 38-55. https://doi.org/10.22115/cepm.2019.160278.1055

[21] Kiyani, K., Raeisi, J., & Heidari, A. (2019). Time-frequency localization of earthquake record by continuous wavelet transforms. Computational Engineering and Physical Modeling, 2(2), 49-61. https://doi.org/10.22115/cepm.2019.193015.1065

[22] Haddad, A., Eidgahee, D. R., & Naderpour, H. (2017). A probabilistic study on the geometrical design of gravity retaining walls. World Journal of Engineering. https://doi.org/10.1108/WJE-07-2016-0034

[23] Shishegaran, A., Taghavizade, H., Bigdeli, A., & Shishegaran, A. (2019). Predicting the Earthquake Magnitude along Zagros Fault Using Time Series and Ensemble Model. Journal of Soft Computing in Civil Engineering, 3(4), 67-77. https://doi.org/10.22115/scce.2020.213197.1152

[24] Ghasemi, S. H., Bahrami, H., & Akbari, M. (2020). Classification of seismic vulnerability based on machine learning techniques for RC frames. Journal of Soft Computing in Civil Engineering, 4(2), 13-21. https://doi.org/10.22115/scce.2020.223322.1186

[25] Nayfeh, A. H. (2008). Perturbation methods. John Wiley & Sons.